Absolute frequency measurements in Yb with 0.08 ppb uncertainty: Isotope shifts and hyperfine structure in the 399-nm $^1S_0 \rightarrow {}^1P_1$ line

Dipankar Das, Sachin Barthwal, Ayan Banerjee, and Vasant Natarajan*
Department of Physics, Indian Institute of Science, Bangalore 560 012, India
(Received 10 September 2004; published 23 September 2005)

We apply our recent technique of using a Rb-stabilized ring-cavity resonator to measure the absolute frequencies of various isotopic components in the 399-nm $^1S_0 \rightarrow {}^1P_1$ line of Yb. For the transition in ^{174}Yb, we obtain a value of 751 525 987.761(60) MHz, representing a relative uncertainty of 0.08 ppb. We also obtain the isotope shifts and hyperfine structure with 50 kHz precision, an order-of-magnitude improvement over our earlier measurements on this line. Our earlier work had helped in resolving some discrepancies among previous measurements, and the present work further confirms those results.

DOI: 10.1103/PhysRevA.72.032506 PACS number(s): 32.30.Jc, 32.10.Fn, 06.30.Ft

I. INTRODUCTION

We have recently developed a technique for measuring the absolute frequencies of optical transitions with uncertainty below 50 kHz [1,2]. The technique uses a ring-cavity resonator whose length is calibrated against a reference laser locked to the D_2 line of ^{87}Rb. The frequency of the reference transition is known with 10-kHz precision, allowing similar high precision in the measurement of the unknown transition. We had earlier applied this technique to the measurement of the 399-nm $^1S_0 \leftrightarrow {}^1P_1$ line in atomic Yb [3]. We used a frequency-doubled Ti:sapphire laser to access the UV line. By measuring the frequency of the IR laser, we were able to avoid several sources of systematic error. We had demonstrated sub-MHz precision in the measurement, and helped in resolving some discrepancies among earlier measurements on this line.

In this paper, we further extend the precision of the measurements by an order of magnitude. The improvement is made possible by two main advances in our technique: we evacuate the cavity to eliminate errors due to dispersion, and we actively lock the Ti:S laser to a given transition. Yb is important because it is an attractive candidate for studying atomic parity violation [4] and the search for a permanent electric-dipole moment in atoms [5]. Laser-cooled Yb has also been proposed for frequency-standards applications [6]. Yb has been recently Bose condensed in an optical trap [7]. The $^1S_0 \leftrightarrow {}^1P_1$ line is widely used in laser-cooling experiments of Yb [8–10]. Over the years, there has therefore been much interest in this line, and its isotopic and hyperfine components have been measured using a variety of techniques—level-crossing and anticrossing spectroscopy [11–13], Fabry-Perot cavity [14], saturated-absorption spectroscopy [15], photon-burst spectroscopy [16], and most recently using optical double-resonance spectroscopy with cold atoms in a magneto-optic trap [9]. However, all these measurements have errors of several MHz and show some discrepancies with each other. In our earlier work [3], we had resolved these discrepancies and the present work further confirms those results.

II. EXPERIMENTAL DETAILS

Our frequency-measurement technique uses the fact that the *absolute* frequency of the D_2 line in ^{87}Rb ($5S_{1/2} \leftrightarrow 5P_{3/2}$ transition) has been measured with an accuracy of 10 kHz [17]. A diode laser locked to this line is used as a frequency reference. A second laser is in turn locked to the unknown transition. The two lasers are coupled into a ring-cavity resonator and the cavity is locked to the unknown laser. At this cavity length, the reference laser will have a small frequency offset from the nearest cavity resonance. The offset is measured and combined with the cavity mode number to obtain a precise value for the *absolute* frequency of the unknown laser. We have already used this technique to make measurements of several IR lines with high precision [1,2,18]. In the current work, we apply the technique for UV measurements using a frequency-doubled IR laser to access the UV line. By measuring the frequency of the IR laser and not the UV laser, we avoid several complications associated with UV frequency measurements. The technique is well suited to the measurement of hyperfine intervals and isotope shifts since several sources of systematic error cancel in such measurements.

A. Schematic

The schematic of the experiment, shown in Fig. 1, is essentially the same as described in our earlier work [3]. Laser1 is a frequency-stabilized diode laser (linewidth <300 kHz) that acts as the frequency reference for the cavity. It is locked to one of the hyperfine transitions in the D_2 line of ^{87}Rb using saturated-absorption spectroscopy in a vapor cell. Laser2 is a tunable Ti:Sapphire (Ti:S) laser (Coherent 899-21) whose output is frequency stabilized to a linewidth of 500 kHz using a temperature-controlled reference cavity. Its output is then frequency doubled to access the 399-nm Yb line. A part of the output is tapped off before the doubler and coupled into the ring-cavity resonator for the frequency measurement.

*Electronic address: vasant@physics.iisc.ernet.in; URL: physics.iisc.ernet.in/~vasant

 ©2005 The American Physical Society

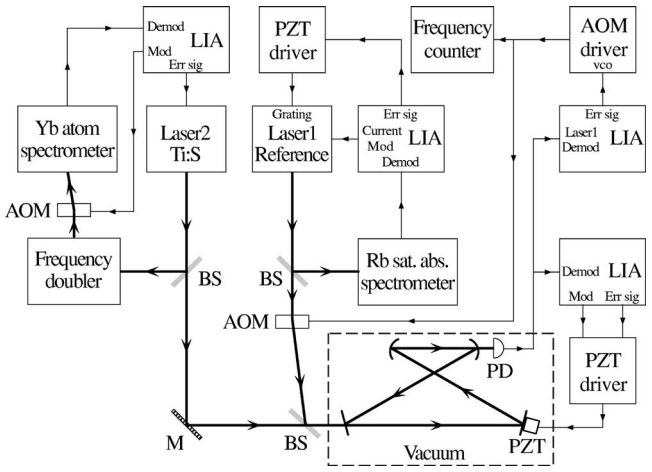

FIG. 1. Schematic of the experiment. Figure key—LIA: lock-in amplifier, PZT: piezoelectric transducer, AOM: acousto-optic modulator, BS: beam splitter, M: mirror, PD: photodiode.

As mentioned earlier, we have made two improvements to the technique since our earlier work. First, we evacuate the cavity to a pressure below 10^{-2} Torr. This eliminates any dispersion effects inside the cavity, and enables us to obtain the absolute frequency. Secondly, the Ti:S laser is actively locked to a given Yb transition using a third-derivative error signal. In the earlier work, the laser was scanned and the peak center was determined by fitting a Lorentzian curve to the measured spectrum.

B. Yb spectroscopy

Yb spectroscopy is done inside a vacuum chamber maintained at a pressure below 10^{-9} Torr. The Yb atomic beam is produced by heating a quartz ampoule containing metallic Yb to a temperature of 400 °C. To reduce Doppler broadening, the laser beam intersects the atomic beam at right angles and the fluorescence from the atoms is detected using a photomultiplier tube through a narrow slit. A typical Yb spectrum is shown in Fig. 2. The laser intensity is about 7 mW/cm^2 compared to the saturation intensity of 68 mW/cm^2. At this intensity, the observed linewidth is 38 MHz, which is only 35% larger than the natural linewidth

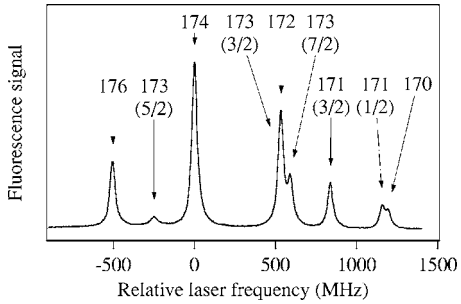

FIG. 2. Yb spectrum. The trace shown is the fluorescence signal for $^1S_0 \rightarrow {}^1P_1$ transitions in the different isotopes of Yb, as labeled. The odd isotopes have hyperfine structure and are labeled with the value of F' in the excited state. Two of the peaks contain overlapping transitions.

of 28 MHz. The various components corresponding to the several stable isotopes are seen in the spectrum. The transition for the rarest isotope, ^{168}Yb, occurs to the right and is not shown because it is not visible on this scale. However, that peak is also visible when the gain of the photomultiplier is increased by a factor of 100.

The Yb spectrum has two peaks where there is significant overlap between neighboring transitions. One of these consists of the ^{171}Yb($F=1/2$) and the ^{170}Yb transitions. This does not present any problem in our technique because the two transitions are separated by about 40 MHz and the spectrum has two clear maxima. The third-derivative locking ensures that we are locked close to the actual line center. This is in contrast to using first-derivative locking where we would lock to the peak in the combined spectrum, which is pulled by the neighboring transition. In addition, the third-derivative signal gives tighter locking and is less sensitive to intensity fluctuations [19].

However, there is some residual effect of the neighboring transition even for third-derivative locking when the peaks are separated by less than 3 linewidths. To determine the size of this shift, we have done computer simulations of two Lorentzian curves separated by 39.5 MHz. We find that the shift of the third-derivative zero from the line center depends on the linewidth. As the linewidth is varied from 35 to 40 MHz (the range of observed linewidths), the shift for the ^{171}Yb($F=1/2$) transition varies from -100 to -170 kHz. Thus, the measured value (which is the location of the third-derivative zero) is shifted by an average amount of $-135(35)$ kHz from the line center, where the additional uncertainty of 35 kHz arises due to the variation in the observed linewidths. The line center is therefore obtained by adding 135(35) kHz to the measured value. Similarly, the line center for the ^{170}Yb transition is obtained by subtracting 167(43) kHz from the measured value.

The other overlapping peak in the Yb spectrum consists of the ^{173}Yb($F=3/2$), the ^{172}Yb, and the ^{173}Yb($F=7/2$) transitions, all lying within 50 MHz of each other. As seen from Fig. 3, the first two transitions are separated by less than the natural linewidth and are completely merged. If we fit a single Lorentzian curve to these two transitions, the fit is quite good (with small residuals) but its linewidth is 1.3 times larger than the linewidth of the neighboring ^{173}Yb($F=7/2$) transition, and indeed the linewidth of all the other peaks in the spectrum. This gives us confidence that the increased linewidth is a result of the convolution of two individual Lorentzians. Computer simulation of the three-transition peak also shows that the location of the third-derivative zeroes are shifted by $-24(18)$ kHz from the ^{172}Yb transition and by $+113(24)$ kHz from the ^{173}Yb($F=7/2$) transition. Therefore, there is no ambiguity in identifying the locations of these transitions. However, as before, the measured frequencies are corrected for this shift.

In order to determine the exact location of the first (unresolved) transition, we fit the observed spectrum to three Lorentzian curves, with the positions of the second and third transition fixed at their measured locations, and the constraint that all three curves have the same linewidth. The fitting algorithm then returns three curves having a linewidth

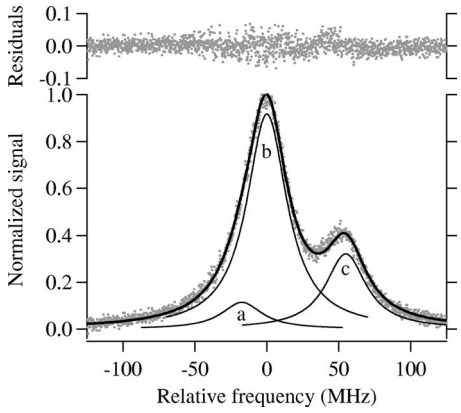

FIG. 3. Three-peak fitting to extract overlapping transitions. The fluorescence signal (shown as gray circles) is fitted to three Lorentzians with the same linewidth. The three peaks correspond to ^{173}Yb($F=3/2$) labeled as (a), ^{172}Yb labeled as (b), and ^{173}Yb($F=7/2$) labeled as (c). The thick line is the sum of the three peaks and fits the measured data quite well as seen from the featureless residuals shown on top.

similar to what we obtain for other well-resolved peaks in the spectrum. As seen from Fig. 3, the fit residuals are very small and their structure-less noise shows that there is little ambiguity in the fitting. After fitting to 15 such spectra, we find that the ^{173}Yb($F=3/2$) transition lies 17.31(20) MHz below the ^{172}Yb transition. In our earlier work, we had used similar fitting to find the separation to be 17.94(90) MHz. The improvement in the current work is mainly because we can fix the exact location of the second and third transitions.

C. Frequency measurement

The frequency measurement proceeds as follows. The outputs of laser 1 (reference) and laser 2 (Ti:S) are coupled into the ring cavity. The cavity length is adjusted using a piezo-mounted mirror to bring it into resonance with the frequency of laser 2. The cavity is then locked to this length in a feedback loop. However, laser 1 will still be offset from the cavity resonance. This offset is accounted for by shifting the frequency of the laser using an acousto-optic modulator (AOM) before it enters the cavity. The frequency of the AOM is then locked to the offset by feeding back the error signal to the AOM driver. Thus, the cavity is simultaneously in resonance with the frequency of laser 2 and the shifted frequency of laser 1. Once the exact cavity length (or mode number) is known, the known frequency of laser 1 is used to determine the absolute frequency of laser 2.

The measurement relies on the fact that the cavity mode number is known exactly. This is done in two steps: we first measure the cavity free-spectral range (FSR) and then use a coarse measurement of the frequency of laser 2. The FSR measurement proceeds as follows. We lock the reference laser to the $F=2\rightarrow F'=(2,3)$ transition and measure the AOM offset for the ^{174}Yb transition. We then shift the reference laser to the $F=1\rightarrow F'=(1,2)$ transition, which is exactly 6622.887 MHz higher [17,20]. This shift causes the cavity mode number to increase by almost exactly 5 since the FSR is about 1325 MHz. The cavity is then used to measure the new AOM offset for the same ^{174}Yb transition. Since the cavity length in both cases is locked to the same transition and remains unchanged, the difference in the two AOM offsets along with the change in the reference frequency gives exactly 5 times the cavity FSR. Using this method, the FSR is determined with a precision of 20 kHz.

The next step in determining the mode number is to get a coarse measurement of laser 2. For this, we use a homebuilt wavemeter [21] that gives the frequency with an uncertainty of 20 MHz. Thus, there is a unique mode number that matches the resonance condition for the two laser frequencies and the measured FSR. For example, the next-nearest mode satisfying the resonance has an FSR differing by 450 kHz, or 22 times the error in the determination of the FSR. Similarly, a change in the mode number by one causes the frequency of the ^{174}Yb transition to change by 60 MHz, or about 3 times the error with which the frequency is known.

III. ERROR ANALYSIS

The errors in our technique have been discussed extensively in earlier publications [1–3,18] and are reviewed here for completeness. The errors that are particular to the Yb line are discussed in greater detail below.

A. Statistical errors

The primary sources of statistical error in our technique are fluctuations in the lock points of the reference and the Ti:S lasers, and the locking of the cavity and the AOM. To minimize such effects, we use an integration time of 10 s in the frequency counter during each measurement of the AOM offset. We then take an average of about 50 measurements for a given transition. This results in an overall statistical error of less than 10 kHz in each measurement.

B. Systematic errors

There are two kinds of potential systematic errors that we have considered. The first class of errors comes from systematic shifts in the laser frequencies. The second class of errors is inherent to our technique because we are really comparing the wavelength (and not the frequency) of the two lasers, and hence we have to account for possible dispersion effects. Let us first consider the shift in the lock points of the lasers.

1. Shift of the reference laser

(i) Shift in the peak position can occur due to (a) optical-pumping effects and (b) velocity redistribution of the atoms in the vapor cell due to radiation pressure [22]. Such effects manifest themselves as inversion of hyperfine peaks or distortion of the Lorentzian line shape. We minimize these effects by carefully adjusting the intensities of the pump and probe beams in the saturated-absorption spectrometer to get narrow and symmetric line shapes.

(ii) Shift in the lock point of the laser due to peak pulling from neighboring transitions, the underlying Doppler profile, or phase shifts in the feedback loop. We minimize these ef-

fects by using third-harmonic detection for the error signal [19].

(iii) Shifts due to collisions in the vapor cell. In Rb, the density inside the cell is $\sim 10^9$ atom/cc, and we estimate the shift to be less than 10 kHz.

(iv) Line shifts from magnetic-field inhomogeneity in the vicinity of the cells. For Rb, the effects are negligible at the values of field inhomogeneity in the laboratory. We further verify this by repeating the experiment by placing the cell at different locations in the laboratory.

One check for the above effects is the linewidth obtained in the saturated-absorption spectrum. For Rb, the observed linewidth is about 12–15 MHz compared to the natural linewidth of 6 MHz. The primary cause for this increase is power broadening by the pump laser and a small misalignment angle between the counter-propagating beams. To confirm this, we have studied the variation of the linewidth as a function of pump power. With near-perfect alignment of the beams and with a magnetic shield [23] around the cell, the linewidth extrapolated to zero power is only 6.5 MHz. This shows that collisional broadening in the vapor cell is negligible. The effect of stray magnetic fields in the vicinity of the cell is to increase the linewidth by 15–20 %. In earlier work, we have shown that the reference laser, after taking into account the above effects, is locked to line center with an uncertainty below 30 kHz.

2. Shift of the Yb laser

Many of the effects discussed above are negligible for the Yb line because we do spectroscopy using an atomic beam. For example, collisional shifts in an atomic beam are insignificant. In addition, the even isotopes have no hyperfine structure and optical pumping effects are nearly absent. This is confirmed by the fact that the relative amplitudes of the even isotopes in the spectrum exactly matches their relative abundance.

The primary source of systematic shift in the Yb spectrum arises due to improper perpendicular alignment of the laser beam with the Yb atomic beam. A misalignment angle of 1 mrad will cause a Doppler shift of about 700 kHz. To minimize this effect, we repeat each measurement with a counterpropagating laser beam. Since the Doppler shift with this beam is of opposite sign, the error cancels when we take an average of the two values. Indeed, the difference between the two values gives an estimate of the misalignment angle, which in our case is less than 0.4 mrad (shift below 300 kHz). In any case, the error cancels in the determination of the isotope shifts (relative to ^{174}Yb) since all isotopes experience the same shift. There is a small differential Doppler shift due to the fact that the different isotopes leave the oven with slightly different velocities. But even for a large misalignment angle of 1 mrad the differential shift is only 12 kHz, which is negligible at our level of precision.

As discussed earlier, there is a small shift of the line center from the third-derivative zero for the overlapping transitions. The frequencies for these transitions have been corrected for the corresponding shifts. However, the additional error in determining the size of the shift is incorporated into the total error for these transitions.

3. Dispersion effects

One potential source of systematic error arising due to dispersion of the medium inside the cavity is eliminated by using an evacuated cavity. However, there could be wavelength-dependent phase shifts at the dielectric-coated mirrors used in the cavity. This error can be checked by repeating the measurement at different cavity lengths. We have shown earlier that the error is negligible in the measurement of the Rb D_1 line at 795 nm [2]. We have recently measured the D lines of Cs [18], which differ by up to 115 nm from the reference transition, and again this error is negligible. Therefore, the current work was done at a single cavity length. It is also important to note that this class of wavelength-dependent systematic errors does not affect the determination of frequency differences of the unknown laser, up to several 10 s of GHz. Thus, in the measurement of the Yb line, this error would cause all the measured frequencies to shift, but the isotope shifts listed in Table I will not change down to the 1 kHz level.

4. Diffraction effects

Diffraction effects inside the cavity appear as an additional (Guoy) phase as the beam propagates through a cavity waist. These effects can be quite important in interferometers and wavemeters. The Guoy phase is given by [24] $\arctan(z/z_R)$, where z is the propagation distance and $z_R = \pi w_0^2/\lambda$ is the Rayleigh range around a waist of radius w_0. In our cavity, the *ABCD* matrix analysis shows that the two waist sizes are proportional to $\sqrt{\lambda/\pi}$ [25]. Therefore, the Rayleigh ranges are identical for all wavelengths, and so is the Guoy phase. In effect, the concave mirrors in the cavity impose a boundary condition on the wavefront curvature at their locations, and this ensures that the Rayleigh ranges are independent of wavelength. Thus one does not expect any systematic error due to this effect.

5. Other effects

An important source of error in wavemeters based on a scanning Michelson interferometer, as described in our earlier work [21], is the geometric alignment of the reference and unknown beams into the interferometer. Any misalignment angle between the beams would change the measured wavelength. By contrast, the cavity technique used in the current work is completely insensitive to geometric factors. The geometric alignment of the beam determines (very sensitively) the degree of mode matching into the cavity, but the cavity resonance condition depends only on the wavelength. Furthermore, we check the mode structure to verify that no higher-order cavity modes are excited [18], which could cause peak pulling of the fundamental mode.

As another check on such errors, we have measured the same Yb transition using different hyperfine transitions to lock the reference laser. The reference frequency changes by known amounts (up to several GHz), and we have verified that the measured frequencies are consistent within the error bars. Changing the lock point of the reference laser changes the cavity mode number and the AOM offset needed to bring it into resonance with the cavity. This checks for geometric

TABLE I. Listed are the frequencies of various transitions in the 399-nm $^1S_0 \leftrightarrow {}^1P_1$ line in Yb. The frequency of the transition in ^{174}Yb is 751 525 987.761(60) MHz, and the other frequencies are listed as shifts from this transition. The values reported in our earlier work are listed alongside.

	Shift from ^{174}Yb (MHz)					
Isotope	This work	Ref. [3]	Ref. [9]	Ref. [16]	Ref. [14]	Ref. [26]
^{176}Yb	−509.310(50)	−509.98(75)	−507.2(25)		−509.4(40)	−469.20(27)
^{173}Yb ($F=5/2$)	−253.418(50)	−254.67(63)				
^{173}Yb ($F=3/2$)	515.975(200)	516.26(90)				
^{172}Yb	533.309(53)	533.90(70)	527.8(28)		529.9(40)	530.2(78)
^{173}Yb ($F=7/2$)	587.986(56)	589.00(45)	578.1(58)			
^{171}Yb ($F=3/2$)	832.436(50)	833.24(75)	832.5(56)	834.4(40)		
^{171}Yb ($F=1/2$)	1153.696(61)	1152.86(60)	1151.4(56)	1136.2(58)		
^{170}Yb	1192.393(66)	1192.48(90)	1175.7(81)	1172.5(57)	1195.0(108)	1158.9(114)
^{168}Yb	1887.400(50)	1886.57(100)		1870.2(52)		
^{173}Yb (centroid)	291.516(54)	291.61(35)			291.2(100)	
^{171}Yb (centroid)	939.523(39)	939.78(54)	938.8(42)	935.0(33)	943.7(70)	

alignment errors since the direction of the beam entering the cavity varies with the AOM frequency.

IV. RESULTS

The measured frequencies of the various transitions in the $^1S_0 \leftrightarrow {}^1P_1$ line of Yb are listed in Table I. Though the absolute frequency of each transition has been measured, the values are listed as shifts from the ^{174}Yb transition. This allows direct comparison with earlier work where only the shifts were measured. The frequency of the ^{174}Yb transition is

$$6s6p\,{}^1P_1 - 6s^2\,{}^1S_0{:}751\,525\,987.761(60)\ \text{MHz}.$$

The frequency is the average value from 12 independent measurements (with independent realignment of the laser beam with respect to the atomic beam, realignment of the AOMs, etc.), repeated over a period of several weeks, and obtained with different lock points of the reference laser. The statistical variation in the average is only 15 kHz. The final error of 60 kHz is the total error taking into account all the sources of systematic error.

The frequency of all the other components in the spectrum are measured with the same accuracy of 60 kHz, and can be obtained by adding the corresponding isotope shift to the above frequency. Note that the isotope shifts have an error of only 50 kHz because several sources of systematic error cancel in determining the difference. For example, the error due to misalignment of the Yb beam with the laser beam is negligible. Thus, we find that the difference in the frequency measured with the right-traveling beam and the left-traveling beam is about +600 kHz for the various transitions, but only ±50 kHz for the isotope shifts. Similarly, any systematic shift in the lock point of the reference laser does not affect the isotope shift. Four of the transitions that have to be corrected for peak pulling have slightly larger errors due to the additional uncertainty in determining the correction. The unresolved ^{173}Yb($F=3/2$) transition has an error of 200 kHz from the three-peak fitting, as discussed earlier.

Also listed in the table are results from our earlier work on this line with sub-MHz precision [3], and other previous measurements. It is clear that our earlier work had already resolved the discrepancies among the previous measurements. For ^{176}Yb, the low value obtained by Chaiko [26] appeared to be incorrect. For ^{171}Yb($F=1/2$), we were in better agreement with the value of 1151.4 MHz reported by Loftus *et al.* [9] using laser-cooled atoms. For ^{170}Yb, we were close to the value reported by Grundevik *et al.* [14], and again the value obtained by Chaiko [26] appeared to be incorrect. The current values further verify those results since they are completely consistent with our earlier work, but the accuracy is improved by an order of magnitude.

Hyperfine structure in ^{171}Yb *and* ^{173}Yb. We have used the data in Table I to obtain the hyperfine-coupling constants in the $6s6p\,{}^1P_1$ state of the odd isotopes ^{171}Yb and ^{173}Yb. For ^{171}Yb, the measured $\{3/2-1/2\}$ interval is used to calculate the magnetic-dipole coupling constant A, yielding a value of

$$A_{171} = -214.173(53)\ \text{MHz}.$$

This value is compared with earlier values in Fig. 4. Our

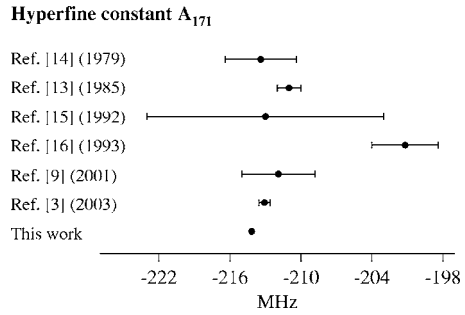

FIG. 4. Hyperfine structure in ^{171}Yb. The figure shows a comparison of our value of the hyperfine constant A_{171} with earlier values.

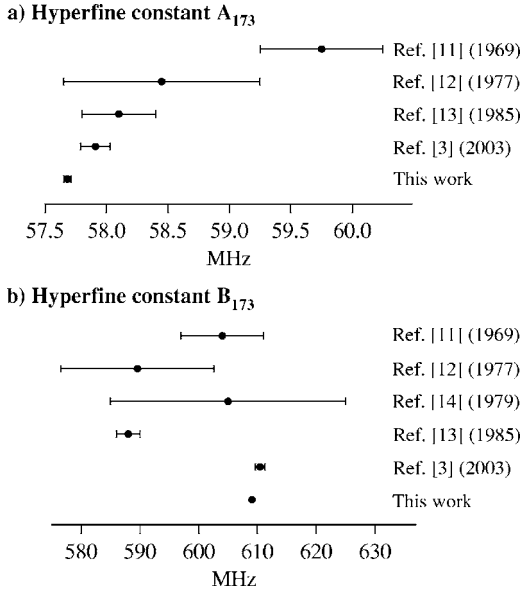

FIG. 5. Hyperfine structure in ^{173}Yb. The figure shows a comparison of our values of the hyperfine constants with earlier values: of A_{173} in (a) and of B_{173} in (b).

value is consistent but has significantly smaller error.

For ^{173}Yb, there are three hyperfine levels and the measured intervals are used to calculate the magnetic-dipole coupling constant A and the electric-quadrupole coupling constant B. We obtain values of

$$A_{173} = 57.682(29)\ \text{MHz},$$

$$B_{173} = 609.065(98)\ \text{MHz}.$$

These values are compared to earlier results in Figs. 5(a) and 5(b), respectively. While our value of A_{173} is consistent, the value of B_{173} is higher than the value reported by Liening [13] from a level-crossing experiment. However, our value is in agreement with the other values, and our earlier measurement.

V. CONCLUSIONS

In conclusion, we have measured the absolute frequencies of various components in the 399-nm $^1S_0 \rightarrow {}^1P_1$ line in Yb. The frequencies are measured using our recently developed technique of using a ring-cavity resonator stabilized to the D_2 line of Rb. The UV line in Yb is accessed with a frequency-doubled IR laser. By measuring the frequency of the IR laser instead of the UV laser, we extend our technique to the measurement of UV frequencies without the concomitant dispersion errors that might occur when comparing UV frequencies against the IR reference. In addition, the technique becomes simpler because the optics used (in both the wavemeter used for the coarse frequency measurement and the ring-cavity used for the final measurement) does not have to cover the UV to IR range. We obtain 60-kHz precision in the determination of the frequency of the transition in ^{174}Yb, and 50-kHz precision in the determination of the isotope shifts for all isotopes including the rarest isotope ^{168}Yb. This represents more than an order-of-magnitude improvement over our earlier work on this line, and is achieved by actively locking the laser to the various transitions. We also obtain improved values for the hyperfine constants in the $^1P_1$ state of the odd isotopes. In future, we plan to apply the frequency-measurement technique to determine isotope shifts and hyperfine structure in the $^1S_0 \rightarrow {}^3P_1$ ultranarrow intercombination line of Yb at 556 nm. This line is important in laser-cooling experiments, and the nearby metastable $^3P_0$ state has applications in optical frequency standards.

ACKNOWLEDGMENTS

This work was supported by the Department of Science and Technology, Government of India. Two of us (D.D. and S.B.) acknowledge financial support from the Council of Scientific and Industrial Research, India.

[1] A. Banerjee, D. Das, and V. Natarajan, Opt. Lett. **28**, 1579 (2003).
[2] A. Banerjee, D. Das, and V. Natarajan, Europhys. Lett. **65**, 172 (2004).
[3] A. Banerjee *et al.*, Europhys. Lett. **63**, 340 (2003).
[4] D. DeMille, Phys. Rev. Lett. **74**, 4165 (1995).
[5] V. Natarajan, Eur. Phys. J. D **32**, 33 (2005).
[6] J. L. Hall, M. Zhu, and P. Buch, J. Opt. Soc. Am. B **6**, 2194 (1989).
[7] Y. Takasu *et al.*, Phys. Rev. Lett. **90**, 023003 (2003).
[8] K. Honda *et al.*, Phys. Rev. A **59**, R934 (1999).
[9] T. Loftus, J. R. Bochinski, and T. W. Mossberg, Phys. Rev. A **63**, 023402 (2001).
[10] U. D. Rapol, A. Krishna, A. Wasan, and V. Natarajan, Eur. Phys. J. D **29**, 409 (2004).
[11] B. Budick and J. Snir, Phys. Rev. **178**, 18 (1969).
[12] M. Baumann, H. Leining, and H. Lindel, Phys. Lett. **59A**, 433 (1977).
[13] H. Liening, Z. Phys. A **320**, 363 (1985).
[14] P. Grundevik, M. Gustavsson, A. Rosen, and S. Rydberg, Z. Phys. A **292**, 307 (1979).
[15] R. W. Berends and L. Maleki, J. Opt. Soc. Am. B **9**, 332 (1992).
[16] K. Deilamian, J. D. Gilaspy, and D. E. Kelleher, J. Opt. Soc. Am. B **10**, 789 (1993).
[17] J. Ye, S. Swartz, P. Jungner, and J. L. Hall, Opt. Lett. **21**, 1280 (1996).
[18] D. Das, A. Banerjee, S. Barthwal, and V. Natarajan, Phys. Rev. A (to be published).
[19] A. J. Wallard, J. Phys. E **5**, 926 (1972).
[20] E. Arimondo, M. Inguscio, and P. Violino, Rev. Mod. Phys. **49**, 31 (1977).
[21] A. Banerjee, U. D. Rapol, A. Wasan, and V. Natarajan, Appl.

Phys. Lett. **79**, 2139 (2001).
[22] R. Grimm and J. Mlynek, Appl. Phys. B: Lasers Opt. **49**, 179 (1989).
[23] Conetic AA Alloy, Magnetic Shield Corporation, Illinois, U.S.A.
[24] A. E. Siegman, *Lasers* (Oxford University Press, Oxford, 1986).
[25] A. Banerjee, Ph.D. thesis, University of Bangalore, India (2004)
[26] Y. Chaiko, Opt. Spectrosc. **20**, 424 (1966).